BIOLOGICAL SCIENCES: Cell Biology

Molecular basis of fatty acid selectivity in the zDHHC family of *S*-acyltransferases revealed by click chemistry

Short title: *Fatty acid selectivity of zDHHC S-acyltransferases*

Jennifer Greaves[1], Kevin R. Munro[2], Stuart C. Davidson[2], Matthieu Riviere[2], Justyna Wojno[2], Terry K. Smith[3], Nicholas C.O. Tomkinson[2], Luke H. Chamberlain[1]

[1]Strathclyde Institute of Pharmacy and Biomedical Sciences, University of Strathclyde, 161 Cathedral Street, Glasgow G4 0RE, UK.
[2]WestCHEM, Department of Pure and Applied Chemistry, University of Strathclyde, 295 Cathedral Street, Glasgow G1 1XL, UK.
[3]BSRC, Schools of Biology and Chemistry, University of St. Andrews, North Haugh, St. Andrews, Fife KY16 9ST, UK.

Correspondence to Luke H. Chamberlain: luke.chamberlain@strath.ac.uk

Keywords: *S*-acylation, palmitoylation, zDHHC, click chemistry, fatty acid, acyl-CoA

Abstract

***S*-acylation is a major post-translational modification, catalysed by the zDHHC enzyme family. *S*-acylated proteins can be modified by different fatty acids; however, very little is known about how zDHHC enzymes contribute to acyl chain heterogeneity. Here, we employed fatty acid azide/alkyne labelling of mammalian cells, showing their transformation into acyl-CoAs and subsequent click chemistry-based detection, to demonstrate that zDHHC enzymes have marked differences in their fatty acid selectivity. This was apparent even for highly related enzymes such as zDHHC3 and zDHHC7, which displayed a marked difference in ability to use C18:0 acyl-CoA as a substrate. Furthermore, we identified Isoleucine-182 in the third transmembrane domain of zDHHC3 as a key determinant limiting the use of longer chain acyl-CoAs by this enzyme. This is the first study to uncover differences in the fatty acid selectivity profiles of cellular zDHHC enzymes and to map molecular determinants governing this selectivity.**

Significance Statement

S-acylation, the attachment of different fatty acids onto cysteine residues, regulates the activity of a diverse array of cellular proteins. This reversible post-translational modification is essential for normal physiology and defects are linked to human disease. S-acylation is catalysed by a large family of "zDHHC" S-acyltransferases that use a cellular pool of diverse fatty acyl-CoAs as substrates. Using chemically-synthesised probes, we show that individual zDHHC enzymes have marked differences in fatty acid selectivity, and identify the underlying molecular basis for this. The study describes how acyl chain heterogeneity of S-acylated proteins is generated, and is significant because the chemical nature of the attached S-acyl chain can fundamentally impact protein behaviour.

Introduction

S-acylation is a reversible post-translational modification (PTM) involving the attachment of fatty acids onto cysteine residues(1, 2). This PTM occurs on both soluble and transmembrane (TM) proteins and exerts a number of important effects, such as mediating membrane binding (of soluble proteins or soluble loops of TM proteins), regulating protein trafficking and targeting to cholesterol-rich membrane micro-domains, and modulating protein stability(3, 4). These actions of *S*-acylation on a diverse array of cellular proteins impact on many important physiological processes, and defects in this process are linked to a number of major diseases and disorders(2, 5).

S-Acylation is mediated by the opposing actions of acyltransferases and thioesterases. *S*-Acyltransferase enzymes belong to the zDHHC protein family, which are encoded by twenty-four distinct genes(6-8). zDHHC enzymes are thought to share the same overall membrane topology, with 4-6 transmembrane domains and the N- and C-termini present in the cytosol(9). The catalytic DHHC cysteine-rich domain (CRD) of the enzymes lies in a cytosolic loop(9) allowing zDHHC enzymes to modify substrate cysteines present at the cytosol-membrane interface. The *S*-acylation reaction is thought to proceed through an enzyme-acyl intermediate, where the acyl chain is attached to the cysteine of the DHHC motif via a thioester linkage (often referred to as enzyme "autoacylation")(10, 11). The *S*-acyl chain is then transferred to a cysteine residue of a substrate protein(10, 11). This overall process is referred to as a "ping-pong" reaction mechanism. There has been progress identifying the zDHHC enzymes that are active against many substrate proteins(2), although we lack a detailed understanding of the protein substrate profiles of individual enzymes and how enzyme-substrate interaction specificity is achieved. Co-expression experiments have suggested that individual zDHHC enzymes might exhibit a level of overlap in their protein substrate profiles, suggesting some possible redundancy within the zDHHC family. Nevertheless, individual enzymes have been linked with many disorders, including schizophrenia, intellectual disability, diabetes and cancer, suggesting that any functional redundancy is limited(2).

In contrast to the steadily increasing knowledge about the specific interactions of individual zDHHC enzymes with their protein substrates, we know relatively little about the fatty acid selectivity of these enzymes. The term *palmitoylation* is often used as a synonym for *S*-acylation. However this does not reflect the potential diversity of *S*-acyl chains added to substrate proteins. Indeed, an analysis of the acyl groups added to *S*-acylated proteins in platelets revealed that 74% were from palmitate (C16:0), 22% from stearate (C18:0) and 4% from oleate (C18:1)(12). Other studies have shown that *S*-acylated proteins can be modified by acyl chains from myristic acid (C14:0), palmitoleic acid (C16:1), linoleic acid (C18:2) and arachidonic acid (C20:4)(12-15). Furthermore, mass spectrometry analysis of the *S*-acyl chains attached to influenza haemagglutinin proteins has revealed that C16:0 and C18:0 fatty acids are attached in a site-specific manner(16). There is also potential for cell type specific differences in the fatty acid profiles of *S*-acylated proteins; for example, one study reported that in RAW26.7 cells less than 10% of the acyl-CoAs were greater than C20, whereas in MCF7 cells C24:0 and C26:0 acyl-CoAs were present at similar amounts to C16:0 and C18:0 acyl-CoAs(17). The identity of the added acyl chain is central to the regulatory effects of *S*-acylation as different acyl chains vary in affinity for membranes and for cholesterol-rich membrane micro-domains(18).

To-date, a single study has explored the potential role of zDHHC enzymes in differential protein *S*-acylation using purified recombinant zDHHC enzymes in detergent micelles(10). This study reported that zDHHC2 catalysed the *S*-acylation of substrate proteins with similar efficiency using palmitate (C16:0), stearate (C18:0) or C20 (C20:0, C20:4) fatty acids. In contrast, zDHHC3 displayed a marked preference for shorter chain length acyl-CoAs and incorporated C16:0 much more efficiently than either C18:0 or C20 fatty acids(10). This elegant study highlighted the potential for discrete patterns of fatty acid selectivity in the zDHHC family, but these questions have been challenging to address, particularly in a cellular context. However, recent developments at the chemistry-biology interface have identified new approaches to investigate this poorly defined area of the *S*-acylation field. Specifically, azide and alkyne fatty acid probes have provided novel and highly-sensitive chemical tools to interrogate S-acylation by click chemistry(19-24). In this study, we report the use of chemically-synthesised azide and alkyne fatty acid probes to investigate fatty acid selectivity in the zDHHC enzyme family and determine the molecular mechanisms governing this specificity.

Results

Synthesised azide fatty acids are good mimics of endogenous fatty acids

Fatty acid azide probes of different acyl chain length were synthesised as described in Supplementary Information. To assess their ability to be taken up by cells, the total fatty acid content of HEK293T cells treated with these synthesised azide fatty acids was determined (Figure 1). Untreated cells showed the expected range of saturated and unsaturated fatty acids, with C18:0 and C18:1 being the most abundant. Upon addition of the various azide fatty acids to the cells, it can clearly be seen that these were not only accumulated within the cells (with C16:0 and C18:0 azides being taken up significantly better than C14:0 and C20:0 azides), but also metabolised by the cells. For example the C16:0 azide was elongated to C18:0, which was subsequently desaturated to

C18:1, while the added C18:0 azide was also desaturated to C18:1 and to a very minor extent C18:2. However, C18:0 azide was not significantly elongated to C20:0, and the added C20:0 azide was neither elongated, nor desaturated (data not shown). This is not surprising as the respective elongase has a high preference for C20:4 to C22:5 and the desaturase has a high selectivity for C18:0(25).

As *S*-acylation of proteins involves acyl-CoA donors, it was deemed important that the impact on the cellular acyl-CoA pools be determined. This was achieved using a multiple reaction monitoring mass spectrometric method in conjunction with an internal non-natural (C17:0) acyl-CoA standard. This analysis revealed that in the untreated HEK293T cells, the C18:1- and C16:0-CoAs were the most abundant, accounting for almost half of the total acyl-CoA pool (Figure 2). Upon addition of the various azide fatty acids, a significant amount of the corresponding acyl-CoA azides were formed, including some of the corresponding metabolised (elongated and desaturated) acyl-CoAs azides, reflecting the total fatty acid content. It is interesting to note that there were decreases in the corresponding endogenous acyl-CoA pools, suggesting clear competition for the acyl-CoA synthases that have a preference for particular acyl chain length.

Collectively, these data strongly suggest that the synthesised azide fatty acids are good mimics of the natural saturated fatty acids and can be used for downstream metabolic processes involving fatty acids, such as lipid metabolism and protein lipidation.

zDHHC enzymes display marked differences in fatty acid azide selectivity in cell-based substrate *S*-acylation assays

To test the ability of the synthesised azide fatty acid probes to reliably measure protein *S*-acylation, HEK293T cells were co-transfected with EGFP-SNAP25b and HA-zDHHC3 or an inactive mutant of this enzyme (C157S). Figure 3A shows that zDHHC3 promoted a marked increase in incorporation of the azide probes into SNAP25, whereas in the absence of active enzyme (either empty vector or the C157S mutant) only a low signal was detected, presumably representing SNAP25 that is modified by endogenously-expressed zDHHC enzymes. To test if the incorporated azide probes were attached to SNAP25 via thioester linkage, transfected cells were treated overnight with 1M hydroxylamine (HA) pH 7, which led to a marked loss of labelling, whereas incubation with 1M Tris (pH 7) as a control had no effect (Figure 3B).

The results presented in Figure 3 suggest that the level of C18:0 incorporation into SNAP25 by zDHHC3 is markedly lower than C14:0 and C16:0. Our previous work and others' has shown that five zDHHC enzymes are active against SNAP25 in similar co-expression assays: zDHHC2, zDHHC3, zDHHC7, zDHHC15 and zDHHC17(26). Thus, we undertook a quantitative comparison of SNAP25 *S*-acylation by these five zDHHC enzymes to examine for the first time if zDHHC enzymes exhibit any differences in fatty acid selectivity when expressed in cells. The results shown in Figure 4A (*top panel*) confirm that zDHHC3 has a marked preference for C14:0/C16:0 over C18:0-azide. Interestingly, zDHHC7 which is highly related to zDHHC3 at sequence level (67.8% identical for mouse) incorporated C18:0-azide into SNAP25 more efficiently than zDHHC3 did, although there was still a significant reduction in C18:0 incorporation relative to C14:0/C16:0 with this enzyme (Figure 4A, *top panel*). zDHHC2 and zDHHC15, also displayed interesting differences in fatty acid azide selectivity despite being highly related at amino acid level (65.4% identical): zDHHC2 exhibited no significant preference whereas C18:0 incorporation into SNAP25 by zDHHC15 was markedly lower than C14:0/C16:0 azides (Figure 4A, *middle panel*). Finally, zDHHC17 showed a preference for longer chain fatty acids and incorporated C16:0 and C18:0 with higher efficiency than C14:0 (Figure 4A, *bottom panel*). We also synthesised corresponding *alkyne* probe and assayed their incorporation into SNAP25 by zDHHC-3, -7 and -17, which revealed the same distinct profiles as seen with the azide probes (Figure 4B). To avoid confusion, the number of carbon groups given in the name for the alkyne probes reflects those of the fatty acid minus the alkyne group. Thus, C14:0-alkyne is a C14 fatty acid chain plus an alkyne group (16 carbon atoms total). Synthesis of these alkyne probes and their IUPAC nomenclature is given in the Supplementary Information.

To generate a more comprehensive understanding of the limits of zDHHC fatty acid selectivity, we also examined C20:0 and C22:0 azide probes. zDHHC3 showed no difference in ability to transfer C18:0, C20:0 or C22:0 (low incorporation for each), whereas zDHHC7 and zDHHC17 displayed a gradual decline in azide incorporation as chain length was increased (Figure 5A). We also used competition assays to test the ability of unlabelled fatty acids to block C16:0 azide incorporation into SNAP25 by zDHHC3 and zDHHC17. Consistent with the observation that zDHHC3 did not incorporate the C18:0 azide probe with high efficiency, neither stearic acid (C18:0) nor oleic acid (C18:1) could block incorporation of C16:0 azide into SNAP25 catalysed by this enzyme, whereas myristic acid (C14:0), palmitic acid (C16:0) and palmitoleic acid (C16:1) were all effective inhibitors (Figure 5B). In contrast to zDHHC3, stearic acid effectively blocked C16:0 azide incorporation into SNAP25 by zDHHC17, whereas myristic acid and palmitic acid had no significant inhibitory effect (Figure 5B). Furthermore, oleic acid and linoleic acid (C18:2) also blocked incorporation of C16:0 azide, and indeed even arachidonic acid (C20:4) was effective at blocking C16:0 azide incorporation by zDHHC17 (Figure 5B). The inhibitory effects of these longer chain unsaturated fatty acids are interesting given that significant amounts of the respective acyl CoAs are present in HEK293T cells (Figure

2). In contrast, lignoceric acid (C24:0) did not inhibit C16:0 azide incorporation, consistent with the results presented in Figure 5A showing that C22:0 azide displayed a marked reduction in incorporation by zDHHC17 compared with shorter chain azide probes. Autoacylation of all zDHHC enzymes tested was dependent on an intact DHHC motif (Supplementary Figure 1).

Different fatty acid selectivities of zDHHC enzymes corresponds to autoacylation status

The *S*-acylation reaction proceeds via an enzyme-acyl intermediate (referred to as "autoacylation") and is followed by transfer of the acyl chain to a substrate protein(10). We therefore tested if the different substrate *S*-acylation profiles observed in Figures 4 and 5 correspond with the autoacylation status of zDHHC enzymes. Figure 6A reveals that the autoacylation profile of zDHHC-2, -3, -7 and -15 were essentially identical to the profile observed for these enzymes with SNAP25 *S*-acylation (Figure 4). Despite repeated attempts, we were unable to reliably detect autoacylation of zDHHC17 and therefore could not compare the autoacylation profile of this enzyme with its substrate *S*-acylation profile. As enzyme autoacylation reliably reports on fatty acid selectivity of zDHHC enzymes, we extended this analysis to provide a more comprehensive study of the zDHHC family. Further distinct fatty acid azide selectivity profiles were identified for a set of zDHHC enzymes for which autoacylation was readily detectable: zDHHC5 and zDHHC11 exhibited a preference for C14:0/C16:0, zDHHC4 showed no preference for C14:0/C16:0/C18:0 and zDHHC23 displayed a marked preference for C18:0 over C14:0 and C16:0 (Figure 6B).

Differences in fatty acid selectivities of zDHHC3 and zDHHC7 are linked to residues in the third transmembrane domain

To understand how differences in fatty acid selectivity might be encoded at the molecular level, we undertook a systematic domain swapping analysis of zDHHC3 and zDHHC7. These enzymes are highly conserved and thus we reasoned that domain swapping between these two isoforms should be less likely to produce deleterious effects on protein folding than similar analyses of other zDHHC enzymes. zDHHC3 and zDHHC7 exhibited a marked difference in ability to incorporate the C18:0 azide probe (Figure 7A) and therefore we focused on this distinction between these two enzymes. This distinction was observed for SNAP25 *S*-acylation (Figure 4), enzyme autoacylation (Figure 6), and we also confirmed it using a different substrate protein (cysteine-string protein; Supplementary Figure 2a). Furthermore, endogenous proteins showed a similar pattern of labelling (Supplementary figure 2b). zDHHC3 and zDHHC7 consist of four predicted transmembrane domains with cytosolic N- and C-termini and a central intracellular loop containing the 51-amino acid catalytic DHHC-CRD (See Figure 7B). Interestingly, replacing either the N- or C-terminal domain or the DHHC-CRD of zDHHC3 with the same domains from zDHHC7 had no detectable effect on the fatty acid selectivity profile of zDHHC3 (Figure 7C). In contrast, replacing all four transmembrane domains of zDHHC3 with those from zDHHC7 or only the second and third transmembrane domains resulted in a significant increase in C18:0 azide incorporation into SNAP25 by these mutant enzymes (Figure 7D), mirroring the fatty acid profile of zDHHC7 (see Figure 7A). Further analysis revealed that substituting only transmembrane domain three of zDHHC3 with the same domain from zDHHC7 was sufficient to change the C18:0 selectivity profile of zDHHC3 (Figure 7E).

To pinpoint the specific features of TMD3 that are important for dictating the fatty acid selectivity profile of zDHHC3, we compared the amino acid sequences of this domain from zDHHC3 and zDHHC7 (Figure 8A). There are four differences in amino acid sequence between zDHHC3 and zDHHC7 in this region and thus we generated two mutants containing either I182S/L184V or M189L/V190C mutations. Figure 8B shows that the I182S/L184V mutation led to a marked increase in C18:0 azide incorporation into SNAP25 by zDHHC3, whereas the M189L/V190C mutations had no effect. Thus, we subsequently generated single I182S and L184V mutations, which clearly showed that the I182S mutation in zDHHC3 significantly enhanced the level of C18:0 incorporation by zDHHC3 whereas the L184V mutation had no effect (Figure 8C). It is interesting to note that zDHHC7 in *Danio rerio* has an isoleucine rather than a serine residue at this position (see Figure 8A). When autoacylation profiles of zDHHC3 and zDHHC7 from this species were examined, we found no significant difference in C18:0 azide incorporation (Supplementary Figure 3), further supporting the important role played by the I/S residues in determining the fatty acid selectivity profiles of zDHHC enzymes.

Finally, to exclude the possibility that any findings with the fatty acid azide probes were related to the presence of the azide/alkyne group, we examined incorporation of ^{3}H-palmitic acid and [^{3}H]stearic acid into SNAP25 by zDHHC3, zDHHC7 and the zDHHC3 (I182S) mutant. Figure 9 shows that the level of incorporation of [^{3}H]palmitic acid catalysed by these zDHHC enzymes was similar. In contrast, zDHHC7 more effectively incorporated [^{3}H]stearic acid than zDHHC3, and the zDHHC3 (I182S) mutant displayed a significant increase in [^{3}H]stearic acid incorporation compared with wild-type zDHHC3 and to a similar level as seen with zDHHC7. Thus, the results of these experiments fully support the results obtained with the fatty acid azides.

Discussion

This study provides the first analysis of zDHHC enzyme fatty acid selectivity within a cellular context. The only other study to examine how zDHHC enzymes handle acyl CoA substrates explored *S*-acylation by purified zDHHC2 and zDHHC3 in

detergent micelles(10). Jennings and Linder demonstrated that zDHHC3 has a strong preference for C16:0 over C18:0 acyl CoA, whereas zDHHC2 displays no overt preference(10). Importantly, this present study has shown that these differences are also seen when zDHHC2 and zDHHC3 are expressed in mammalian cells. zDHHC3 is Golgi-localised(27), whereas zDHHC2 associates with the plasma membrane and endosomes(28). Therefore, the acyl CoA selectivity profiles of zDHHC2/3 are preserved irrespective of whether the enzymes are in detergent micelles or native membranes and irrespective of localisation to distinct membrane compartments.

S-acylation occurs via a two-step process involving enzyme "autoacylation" and subsequent transfer of the acyl chain onto the substrate protein. zDHHC autoacylation provides a robust measure of fatty acid selectivity as we clearly showed that the autoacylation profile of zDHHC2, -3, -7 and -15 closely matched their respective substrate *S*-acylation profiles. This allowed us to investigate the acyl CoA selectivity of an additional set of enzymes by measuring autoacylation activity. Overall, the results of this part of the study showed that zDHHC-3, -5, -7, -11 and -15 prefer C14/C16 over C18, zDHHC-2 and -4 display no clear fatty acid preference, zDHHC17 prefers C16/C18 over C14, and zDHHC23 exhibits a strong preference for C18. These observations re-emphasise the point made above that acyl CoA specificities do not show any correlation with intracellular localisation, for example, zDHHC-3, -7, -15, -17 and -23 all localise to the Golgi region of cells(27, 29), whereas zDHHC-2 and -5 are localised to the plasma membrane(26), and zDHHC4 is ER-localised(30).

zDHHC-3 and -7 are highly related at the sequence level, co-distribute on Golgi membranes and share many common protein substrates. Yet these enzymes have a significant difference in acyl CoA selectivity, with zDHHC7 having an increased ability to incorporate C18:0 chains relative to zDHHC3. The high sequence conservation of zDHHC-3 and -7 provided an opportunity to undertake a comprehensive domain swapping analysis to pinpoint features that underpin acyl CoA selectivity. This analysis identified a single amino acid in the third transmembrane domain of zDHHC3 as a critical determinant limiting the use of longer chain fatty acids by this enzyme. When Ile-182 was replaced by the serine present at the same position in zDHHC7, a significant increase in the ability of the mutant protein to incorporate C18:0 was noted. We confirmed the importance of this residue using both C16:0/C18:0 azides with click chemistry detection and [^{3}H]palmitic acid/stearic acid labelling. In this regard, it is interesting that neither the azide or alkyne group present on the probes appeared to influence acyl chain selectivity, perhaps suggesting that these chemical groups have a flexible character that does not impede association with the zDHHC enzyme. Consistent with this notion, we also found that the fatty acid azides selectively competed for the formation of endogenous acyl-CoA of the same chain length when added to HEK293T cells. This shows that the azide probes compete with and are very good mimics of endogenous fatty acids, and are therefore excellent chemical biology tools with which to interrogate aspects of fatty acid biology such as *S*-acylation.

Although we performed a comprehensive domain-swapping analysis between zDHHC3 and zDHHC7, the high similarity of these two enzymes means that other factors that are important for acyl chain selectivity could have been missed (since these other factors could be conserved between zDHHC-3 and -7). Nevertheless, the approach taken here provides an important first step towards understanding the basis for acyl CoA selectivity in the zDHHC family, and clearly shows the importance of TMDs in this regard. Interestingly, a lysine was identified in the transmembrane domain of an elongase component of the yeast very long-chain fatty acid synthase complex that was also a key determinant of the final length of fatty acyl CoA chain synthesised by this enzyme complex(31). In addition, a subsequent mutational analysis of the related rat elongases Elovl2 and Elovl5 also highlighted the importance of the transmembrane domains of these enzymes in setting the substrate specificity profiles. Elovl2 is required for synthesis of omega-3 docosahexaenoic acid (DHA; 22:6n-3) as this elongase (but not Elovl5) can elongate docosapentaenoic acid (22:5n-3) to 24:5n-3, a precursor of DHA. This difference in substrate specificity between Elovl2 and Elovl5 was shown to involve a region encompassing transmembrane domains 6 and 7, with a cysteine-to-tryptophan switch in transmembrane domain 7 proving to be particularly important in setting specificity(32).

It is tempting to speculate that the transmembrane domains of zDHHC enzymes form "channels" that accommodate specific acyl CoA molecules. This could involve different transmembrane domains in the same zDHHC molecule or might require dimerization and multimerisation of zDHHC enzymes(33). As isoleucine occupies more space that serine, it is possible that this amino acid in TMD3 of zDHHC3 limits the length of acyl chain that can be accommodated by blocking the acyl-CoA channel. This idea is consistent with the position of the isoleucine residue in zDHHC3, which is present in the middle of TMD3. Indeed, the catalytic DHHC-CRD of zDHHC enzymes is present immediately preceding TMD3, suggesting that the cysteine in the DHHC active site could be positioned close to the channel opening.

Mass spectrometry-based analysis of the lipidation profile of haemaglutinin (HA) from influenza has shown site-specific attachment of palmitate or stearate chains onto this protein(34). Interestingly, C18:0 is added specifically to a cysteine present in the transmembrane domain whereas C16:0 is attached to cysteines in a membrane proximal domain. It is not clear how this highly selective process is achieved but our results suggest that the modified cysteines

in this protein might be targeted by different zDHHC enzymes with distinct acyl CoA specificities. It is also possible that there is sometimes a contribution made by the substrate in determining which fatty acids are attached at specific sites. Thus, for transmembrane proteins, *S*-acylated cysteines are often adjacent to transmembrane domains and it is possible that the sequence of the substrate transmembrane domain affects which fatty acids can be attached to the adjacent cysteine in a similar way as seen here for zDHHC enzymes.

There are two major properties of *S*-acylation that are thought to be central to its various effects on modified proteins: increased hydrophobicity and affinity for cholesterol-rich membranes(3, 35). Hydrophobicity is fundamental to the effects of *S*-acylation on reversible membrane binding of many soluble proteins and in regulating the membrane association of soluble loops of transmembrane proteins(3). Association with cholesterol-rich membranes is thought to influence aspects of protein trafficking and membrane compartmentalisation. It is well established from *in vitro* studies that saturated phospholipids cluster together with cholesterol, whereas unsaturated phospholipids are excluded from these domains(36). Although the effects of saturated versus unsaturated *S*-acyl chains have not been studied in such detail, it is clear that *S*-acylation is a major signal for association with cholesterol-rich domains at least *in vitro*(37). It is likely that the addition of saturated versus unsaturated acyl chains onto proteins have distinct influences on membrane partitioning and subsequent trafficking and function in the cell. Furthermore, the acyl chain added to *S*-acylated proteins is also likely to affect the strength of membrane association. Although it is clear that two tandem lipid modifications (e.g. myristoylation/palmitoylation or prenylation/palmitoylation) provides a strong membrane anchor, a single lipid group (e.g. myristoyl or prenyl) is not sufficient for membrane association in the absence of other signals such as a polybasic region(38). However, single myristate (C14:0), palmitate (C16:0) or stearate (C18:0) groups added to an *S*-acylated protein could have markedly different effects on membrane association. Indeed, it was suggested that stearate has a significantly enhanced strength of interaction with phospholipid membranes compared with palmitate(12).

This study has identified clear differences in the fatty acylation profiles of different zDHHC enzymes and their substrates expressed in HEK293 cells. In future work it will be important to further advance understanding of this area and the functional significance of fatty acid heterogeneity by investigating fatty acid selectivity of endogenous proteins and how this is impacted by a dynamic and heterogeneous acyl CoA pool. The distribution of different pools of acyl-CoAs and their availability for use in *S*-acylation reactions is unclear at this time, and this will be an important area of future investigations.

Materials and Methods

Materials

Mouse monoclonal GFP antibody was from Clontech (CA, USA). Rat high-affinity HA antibody was from Roche (West Sussex, UK). IR-dye conjugated secondary antibodies and alkyne/azide probes were purchased from LI-COR (Cambridge UK). [9,10-^{3}H] palmitic acid and [9,10-^{3}H] stearic acid (specific activity for each 1.11-2.22 TBq/mmol) were from Hartmann Analytic (Braunschweig, Germany). Lipofectamine 2000 was from Invitrogen (Paisley, UK). Oligonucleotide primers were purchased from Sigma (Poole, UK).

Cell culture and transfection

HEK293T cells (obtained from ATCC) were cultured in DMEM supplemented with 10% fetal bovine serum at 37 ^{0}C and in a humidified atmosphere containing 5% CO_2. Cells were plated on 24-well plates and transfected the following day using Lipofectamine 2000 according to the manufacturer's instructions. For substrate *S*-acylation assays, 0.8 μg of EGFP-SNAP25 were co-transfected with 1.6 μg of zDHHC plasmid (in pEF-BOS-HA backbone). For autoacylation assays, 3 μg of zDHHC plasmid was used. Cells were labelled and processed the day after transfection.

Quantification of fatty acids and acyl-CoAs

Cells were collected by centrifugation and washed with serum free DMEM, prior to incubation at 37ºC for 15 min with DMEM only, followed by the addition of defatted BSA coupled to the appropriate fatty acid azide (100 μM final concentration) and incubated for 4 hours at 37ºC. Cells were then harvested by centrifugation and either washed in ice cold PBS and freeze-dried for total fatty acid determination or processed for acyl-CoA extraction (see below).

For total fatty acid determination, the freeze-dried cells were subjected to acid hydrolysis using constant boiling HCl (6 M, 200 μL) vortexing/sonication followed by incubation for 16 h at 110ºC. After cooling, the samples were spiked with 100 pmoles of C17:0 fatty acid (as an internal control) and processed and derivatised to fatty acid methyl esters (FAMEs), prior to analysis by gas chromatography-mass spectrometry (GC-MS) as described previously(39). The individual azide fatty acids were also converted to their corresponding FAMEs and analysed by GC-MS to determine retention time and fragmentation patterns (data not shown).

For acyl-CoA extraction and quantification, the absolute number of cells was determined (typically between 2-4 x 10^{7} cells). Cells were harvested by centrifugation at 15,000 x g for 1 min at room temperature and the supernatant media removed. The pellet was washed briefly with 200 μl of ice-cold PBS and completely lysed with ice-cold TCA (100 μl, 1M) and vortexing, and stored on ice to prevent sample hydrolysis.

The internal standard C17:0-CoA (150 pmol) was added to the lysate and the sample centrifuged (15,000g, 10 min, 4°C). The resulting supernatant was transferred to a fresh pre-cooled tube. EDTA (25 μl, 10 mM, pH 7.0) was added followed by chloroform (50 μL) triethylammonium acetate (50 μl), and the mixture was vortexed and centrifuged (15,000 x g, 10 min, 4°C). The upper phase was carefully removed to a fresh Eppendorf tube, flash frozen in liquid nitrogen and freeze dried. The dried sample was kept at -80°C prior to analysis by electrospray-mass spectrometry (ES-MS), using multiple reaction monitoring (MRM) similar to the method of Haynes et al(17).

Samples were suspended in 15 μl of a 1:2 (v/v) chloroform / methanol and 5 μl of acetonitrile / isopropanol / water (6:7:2) and delivered using a NanoMate (Advion) to a AB Sciex 4000 QTRAP triple quadrupole mass-spectrometry with a nanoelectrospray source, using nitrogen as the collision gas. A MRM approach was utilized to quantify acyl CoA. MRM mass transition (Supplementary Table) for the acyl-CoAs was determined in positive ion mode, (EP 8 eV, CXP 12 eV, an interface temperature of 30°C , gas pressure 0.5 psi and a tip voltage of 1.25-1.5kV, dwell time 500 mS), spectra were acquired for 2 minutes. All MRM data were normalized relative to the internal standard before generating standard curves (0.1-500 pmoles) for the acyl-CoAs (C14:0. C16:0, C17:0, C18:0, C20 and C20:4) which were obtained from either Sigma or Avanti Polar Lipids (Alabaster, AL), allowing their own response factor to be determined. Samples were analysed in the same manner, allowing quantification of the extracted acyl-CoAs.

Cell labelling with fatty acid azide and alkyne probes for analysis of *S*-acylation

HEK293T cells were incubated with 100 μM of the fatty acid azide probes (in DMEM with 1 mg/ml defatted BSA) for 4 hours at 37 ^{O}C. For competition experiments, transfected cells were labelled with 100 μM of the C16:0 azide probe in the presence of a 3-fold excess (300 μM) of the relevant fatty acid. For cell labelling with [^{3}H]palmitic acid and [^{3}H]stearic acid (Hartmann Analytic), transfected cells were incubated in DMEM/BSA containing 0.5 mCi/ml of the tritiated fatty acid probes for 4 hours at 37 ^{O}C.

Detection of fatty acid azide and alkyne probes in *S*-acylated proteins

Cells were washed twice in phosphate-buffered saline (PBS) then lysed on ice in 100 μl of 50mM Tris pH 8.0 containing 0.5% SDS and protease inhibitors (Roche, West Sussex UK). Conjugation of azide or alkyne IR-800 Dye (LI-COR, Cambridge UK) to fatty acid azide or alkyne probes was carried out for 1 hr at room temperature with end-over-end rotation by adding an equal volume (100 μl) of freshly mixed click chemistry reaction mixture containing 10 μM IRDye® 800CW azide or alkyne Infrared Dye, 4 mM $CuSO_4$, 400 μM Tris[(1-benzyl-1*H*-1,2,3-triazol-4-yl)methyl]amine and 8 mM ascorbic Acid in dH_20. Proteins were isolated by acetone precipitation and resuspended in 100 μl SDS sample buffer (50mM Tris pH 8.0, 10% glycerol, 2% SDS and 0.1% bromophenol blue) containing 25 mM DTT. Samples were incubated at 95°C for 5 minutes and 10-15 μl of each sample was resolved electrophoretically on 12% Tris-glycine SDS-PAGE gels.

For detection of [^{3}H] fatty acid probes, cell lysates were resolved by SDS-PAGE and transferred to duplicate nitrocellulose membranes. One membrane was immunoblotted with antibodies recognising the GFP- and HA-tags. The other membrane was exposed to light-sensitive film in the presence of a Kodak Biomax Transcreen LE intensifier screen for detection of [^{3}H] fatty acid probe incorporation.

Generation of mutant zDHHC constructs

The zDHHC3 chimeras containing the N- and C-terminal domains (zDHHC3/CN7) or intracellular domain including the zDHHC cysteine-rich domain of zDHHC7 (zDHHC3/CRD7) were generated within the HA-tagged constructs by inserting *Nhe*1 and *Sal*1 restriction sites at the boundaries of the domains that were swapped (upstream of C47 and F235 in zDHHC3 and C50 and F238 in zDHHC7 for zDHHC3/CN7, and S93 and T176 in zDHHC3 and S96 and T179 in zDHHC7 for zDHHC3/CRD7) by site-directed mutagenesis. The regions were then swapped by restriction/ligation and the *Nhe*1/*Sal*1 restriction sites removed using site-directed mutagenesis. The zDHHC3 chimeras containing the transmembrane domains of zDHHC7 were constructed using GeneArt gene synthesis services (Thermo Fisher Scientific) and sub-cloned into pEF-BOS-HA vector using *Bam*H1 restrictions sites. The transmembrane domains predicted by UniProt were defined as follows: zDHHC3 A48-V68 (TMD1), Y73-S93 (TMD2), F172-F192 (TMD3), I215-F235 (TMD4); zDHHC7 A51-L71 (TMD1), F76-S96 (TMD2), F175-G194 (TMD3), I218-F238 (TMD4). Site-directed mutants were generated using PCR. The validity of all clones was confirmed by sequencing.

Data Quantification and Statistical Analysis

Quantification of all click chemistry experiments was performed by expressing the click signal relative to the corresponding protein signal (immunoblot). For substrate *S*-acylation assays, this was then normalised to control (empty pEF-BOS-HA plasmid). Statistical analysis was performed using a one-way ANOVA with a Tukey post-test using Graphpad Prism software.

Acknowledgements

We are grateful to Mike Shipston and Heather McClafferty (University of Edinburgh) for the plasmid encoding zDHHC23 cysteine mutant. This work was funded by a BBSRC grant (BB/L022087/1) to LHC, NCT and TKS, and Wellcome Trust grant (093228) awarded to TKS. We thank the EPSRC Mass Spectrometry Service, Swansea, for high-resolution spectra.

Author contributions

JG and TKS: conceived and performed experiments, analysed data and wrote the manuscript; KRM, SCD MR and JW: synthesised chemical probes; LHC and NCOT: conceived experiments and wrote the manuscript.

References

1. Smotrys JE & Linder ME (2004) PALMITOYLATION OF INTRACELLULAR SIGNALING PROTEINS: Regulation and Function

doi:10.1146/annurev.biochem.73.011303.073954. *Annual Review of Biochemistry* 73(1):559-587.
2. Chamberlain LH & Shipston MJ (2015) The physiology of protein S-acylation. *Physiological reviews* 95(2):341-376.
3. Salaun C, Greaves J, & Chamberlain LH (2010) The intracellular dynamic of protein palmitoylation. *J Cell Biol* 191(7):1229-1238.
4. Linder ME & Deschenes RJ (2007) Palmitoylation: policing protein stability and traffic. *Nat Rev Mol Cell Biol* 8(1):74-84.
5. Greaves J & Chamberlain LH (2011) DHHC palmitoyl transferases: substrate interactions and (patho)physiology. *Trends Biocehm Sci* 36:245-253.
6. Fukata M, Fukata Y, Adesnik H, Nicoll RA, & Bredt DS (2004) Identification of PSD-95 Palmitoylating Enzymes. *Neuron* 44(6):987-996.
7. Lobo S, Greentree WK, Linder ME, & Deschenes RJ (2002) Identification of a Ras Palmitoyltransferase in Saccharomyces cerevisiae

10.1074/jbc.M206573200. *J. Biol. Chem.* 277(43):41268-41273.
8. Roth AF, Feng Y, Chen L, & Davis NG (2002) The yeast DHHC cysteine-rich domain protein Akr1p is a palmitoyl transferase

10.1083/jcb.200206120. *J. Cell Biol.* 159(1):23-28.
9. Politis EG, Roth AF, & Davis NG (2005) Transmembrane Topology of the Protein Palmitoyl Transferase Akr1

10.1074/jbc.M411946200. *J. Biol. Chem.* 280(11):10156-10163.
10. Jennings BC & Linder ME (2012) DHHC PROTEIN S-ACYLTRANSFERASES USE A SIMILAR PING-PONG KINETIC MECHANISM BUT DISPLAY DIFFERENT ACYL-COA SPECIFICITIES. *Journal of Biological Chemistry*.
11. Mitchell DA, Mitchell G, Ling Y, Budde C, & Deschenes RJ (2010) Mutational analysis of Saccharomyces cerevisiae Erf2 reveals a two-step reaction mechanism for protein palmitoylation by DHHC enzymes. *Journal of Biological Chemistry*.
12. Muszbek L, Haramura G, Cluette-Brown J, Van Cott E, & Laposata M (1999) The pool of fatty acids covalently bound to platelet proteins by thioester linkages can be altered by exogenously supplied fatty acids. *Lipids* 34(0):S331-S337.
13. Hallak H*, et al.* (1994) Covalent binding of arachidonate to G protein alpha subunits of human platelets. *J Biol Chem* 269(7):4713-4716.
14. O'Brien PJ & Zatz M (1984) Acylation of bovine rhodopsin by [3H]palmitic acid. *Journal of Biological Chemistry* 259(8):5054-5057.
15. Veit M, Reverey H, & Schmidt MF (1996) Cytoplasmic tail length influences fatty acid selection for acylation of viral glycoproteins. *Biochem J* 318 (Pt 1):163-172.
16. Brett K*, et al.* (2014) Site-specific S-acylation of influenza virus hemagglutinin: the location of the acylation site relative to the membrane border is the decisive factor for attachment of stearate. *J Biol Chem* 289(50):34978-34989.
17. Haynes CA*, et al.* (2008) Quantitation of fatty acyl-coenzyme As in mammalian cells by liquid chromatography-electrospray ionization tandem mass spectrometry. *J Lipid Res* 49(5):1113-1125.
18. Liang X*, et al.* (2001) Heterogeneous Fatty Acylation of Src Family Kinases with Polyunsaturated Fatty Acids Regulates Raft Localization and Signal Transduction. *Journal of Biological Chemistry* 276(33):30987-30994.
19. Hang HC*, et al.* (2007) Chemical Probes for the Rapid Detection of Fatty-Acylated Proteins in Mammalian Cells. *Journal of the American Chemical Society* 129(10):2744-2745.
20. Charron G*, et al.* (2009) Robust fluorescent detection of protein fatty-acylation with chemical reporters. *J Am Chem Soc* 131(13):4967-4975.
21. Hannoush RN & Arenas-Ramirez N (2009) Imaging the Lipidome: Ï‰-Alkynyl Fatty Acids for Detection and Cellular Visualization of Lipid-Modified Proteins. *ACS Chemical Biology* 4(7):581-587.
22. Hannoush RN & Sun J (2010) The chemical toolbox for monitoring protein fatty acylation and prenylation. *Nat Chem Biol* 6(7):498-506.
23. Yap MC*, et al.* (2010) Rapid and selective detection of fatty acylated proteins using

{omega}-alkynyl-fatty acids and click chemistry. *J. Lipid Res.* 51(6):1566-1580.
24. Hang HC & Linder ME (2011) Exploring protein lipidation with chemical biology. *Chemical reviews* 111(10):6341-6358.
25. Guillou H, Zadravec D, Martin PG, & Jacobsson A (2010) The key roles of elongases and desaturases in mammalian fatty acid metabolism: Insights from transgenic mice. *Prog Lipid Res* 49(2):186-199.
26. Greaves J, Gorleku OA, Salaun C, & Chamberlain LH (2010) Palmitoylation of the SNAP25 protein family: specificty and regulation by DHHC palmitoyl transferases. *Journal of Biological Chemistry*.
27. Greaves J, Salaun C, Fukata Y, Fukata M, & Chamberlain LH (2008) Palmitoylation and Membrane Interactions of the Neuroprotective Chaperone Cysteine-string Protein. *J. Biol. Chem.* 283(36):25014-25026.
28. Greaves J, Carmichael JA, & Chamberlain LH (2011) The palmitoyl transferase DHHC2 targets a dynamic membrane cycling pathway: regulation by a C-terminal domain. *Mol. Biol. Cell* 22(11):1887-1895.
29. Tian L, McClafferty H, Knaus H-G, Ruth P, & Shipston MJ (2012) Distinct Acyl Protein Transferases and Thioesterases Control Surface Expression of Calcium-activated Potassium Channels. *Journal of Biological Chemistry* 287(18):14718-14725.
30. Gorleku OA, Barns A-M, Prescott GR, Greaves J, & Chamberlain LH (2011) Endoplasmic Reticulum Localization of DHHC Palmitoyltransferases Mediated by Lysine-based Sorting Signals. *Journal of Biological Chemistry* 286(45):39573-39584.
31. Denic V & Weissman JS (2007) A molecular caliper mechanism for determining very long-chain fatty acid length. *Cell* 130(4):663-677.
32. Gregory MK, Cleland LG, & James MJ (2013) Molecular basis for differential elongation of omega-3 docosapentaenoic acid by the rat Elovl5 and Elovl2. *J Lipid Res* 54(10):2851-2857.
33. Lai J & Linder ME (2013) Oligomerization of DHHC Protein S-Acyltransferases. *Journal of Biological Chemistry* 288(31):22862-22870.
34. Kordyukova LV, Serebryakova MV, Baratova LA, & Veit M (2010) Site-specific attachment of palmitate or stearate to cytoplasmic versus transmembrane cysteines is a common feature of viral spike proteins. *Virology* 398(1):49-56.
35. Resh MD (2006) Trafficking and signaling by fatty-acylated and prenylated proteins. *Nature Chemical Biology* 2(11):584-590.
36. Brown DA & London E (2000) Structure and Function of Sphingolipid- and Cholesterol-rich Membrane Rafts. *Journal of Biological Chemistry* 275(23):17221-17224.
37. Melkonian KA, Ostermeyer AG, Chen JZ, Roth MG, & Brown DA (1999) Role of lipid modifications in targeting proteins to detergent-resistant membrane rafts. Many raft proteins are acylated, while few are prenylated. *J Biol Chem* 274(6):3910-3917.
38. Shahinian S & Silvius J (1995) Doubly-lipid-modified protein sequence motifs exhibit long-lived anchorage to lipid bilayer membranes. *Biochemistry* 34:3813-3822.
39. Trindade S*, et al.* (2016) Trypanosoma brucei Parasites Occupy and Functionally Adapt to the Adipose Tissue in Mice. *Cell host & microbe* 19(6):837-848.

Figure Legends

Figure 1: Relative percentage of the total fatty acid content of cells with and without treatments of azide-fatty acids.
HEK293T cells were incubated with or without fatty acid azides. Fatty acids released from cellular lipids and protein by acid were then converted to methyl esters and analysed by GC-MS as described in material and methods. Values shown are means ± SEM (n=3).

Figure 2: Quantification of the acyl-CoA content of HEK293T cells with and without treatments of azide-fatty acids.
HEK293T cells were incubated with or without fatty acid azides and acyl-CoAs were then quantified as described in materials and methods. Values shown are means ± SEM (n=3).

Figure 3: *S*-acylation of EGFP-SNAP25B by zDHHC3.
HEK293T cells were transfected with EGFP-SNAP25b and pEF-BOS-HA (*vector*), HA-zDHHC3, or HA-zDHHC(C157S), or were left untransfected. Cells were then incubated with C14:0, C16:0 or C18:0 fatty acid azides for 4h at 37 ºC. Incorporated fatty acid azides were detected by click chemistry using an alkyne-800 infrared dye. Isolated proteins were resolved by SDS-PAGE and transferred to nitrocellulose membranes. Representative images are shown. (a) Upper panel: click chemistry signal. Middle panel: anti-GFP immunoblot. Lower panel: anti-HA immunoblot. *Arrowheads* denote the position of the EGFP-SNAP25 band (top and middle panels) and hA-zDHHC3 band (lower panel). (b) Following click chemistry, samples were incubated in hydroxylamine (+) or Tris (-) to a final concentration of 1M overnight prior to SDS-PAGE. Upper panel: click chemistry signal. Lower panel: anti-GFP immunoblot. Position of molecular weight markers is shown.

Figure 4: *S*-acylation of EGFP-SNAP25B by different zDHHC enzymes.
HEK293T cells were transfected with EGFP-SNAP25B and pEF-BOS-HA (*vector*), HA-zDHHC-2, -3, -7, -15 or -17. Cells were then incubated with C14:0, C16:0 or C18:0 fatty acid azides or alkynes as indicated for 4h at 37 ºC. Fatty acid azides/alkynes were labelled by click chemistry using an alkyne- or azide-800 infrared dye. Isolated proteins were then resolved by SDS-PAGE and transferred to nitrocellulose membranes. (a) *S*-acylation analysis of EGFP-SNAP25B using fatty acid-azides. Representative images are shown in the left panel with position of molecular mass standards indicated; graphs showing mean ± SEM shown are in the right panel. zDHHC3: n = 46; zDHHC7: n = 26; zDHHC2: n= 10; zDHHC15: n = 9; zDHHC17: n = 22. **p < 0.01; ***p < 0.001. (b) *S*-acylation analysis of EGFP-SNAP25B in HEK293T cells labelled with fatty acid-alkynes. Graphs show mean ± SEM (n=10). ns = not significant; **p < 0.01; ***p < 0.001.

Figure 5: *S*-acylation of EGFP-SNAP25B by longer-chain saturated and unsaturated fatty acids.
(a) *S*-acylation analysis of EGFP-SNAP25B by HA-zDHHC3, HA-zDHHC7 and HA-zDHHC17 in HEK293T cells with C14:0, C16:0, C18:0, C20:0 and C22:0 fatty acid-azides. Representative images are shown and position of molecular mass standards indicated. Upper panel: click chemistry signal. Middle panel: anti-GFP immunoblot. Lower panel: quantified data. n ≥ 3, mean ± SEM. (b) Competition analysis of EGFP-SNAP25b *S*-acylation by HA-zDHHC3 (upper panel) or HA-zDHHC17 (lower panel) in HEK293T cells labelled with C16:0-azide in the presence of 3-fold excess of the indicated unlabelled (u) fatty acids. Position of molecular mass standards is shown. Graphs show mean values ± SEM (n ≥ 3). ns = not significant; *p < 0.05; **p < 0.01; ***p < 0.001.

Figure 6: Autoacylation of zDHHC enzymes by fatty-acid azides.
HEK293T cells transfected with HA-tagged zDHHC constructs were incubated with C14:0, C16:0 or C18:0 fatty acid azides for 4h at 37 ºC. Fatty acid azides were then labelled by click chemistry using an alkyne-800 infrared dye. Isolated proteins were resolved by SDS-PAGE and transferred to nitrocellulose membranes. Representative click signals and western blots with position of molecular mass standards indicated, together with quantified data (mean ± SEM) are shown for each zDHHC enzyme. (a) Autoacylation of zDHHC enzymes active against SNAP25B. zDHHC2: n = 6; zDHHC3: n = 14; zDHHC7: n = 11; zDHHC15: n = 6. (b) Autoacylation of additional zDHHC enzymes. n ≥ 6. ns = not significant; *p < 0.05; **p < 0.01; ***p < 0.001. The arrowhead on the zDHHC5 blot indicates the zDHHC5 band.

Figure 7: *S*-acylation of EGFP-SNAP25B by zDHHC3/zDHHC7 chimeras.
HEK293T cells were transfected with EGFP-SNAP25B and pEF-BOS-HA (*vector*) or the indicated wild-type or mutant zDHHC constructs. Cells were then incubated with C14:0, C16:0 or C18:0 fatty acid azides for 4h at 37 ºC. Fatty acid azides were labelled by click chemistry using an alkyne-800 infrared dye. Isolated proteins were then resolved by SDS-PAGE and transferred to nitrocellulose membranes for analysis. (a) Quantification of the relative levels of C14:0-, C16:0- or C18:0-azide incorporation into EGFP-SNAP25B

by zDHHC3 or zDHHC7 (mean ± SEM). n ≥ 26. (b) Schematic illustration detailing the zDHHC3/zDHHC7 chimeras that were constructed. (c-e) Analysis of EGFP-SNAP25B *S*-acylation by zDHHC3 chimeras with fatty acid-azides. Representative images are shown on the left, graphs showing mean ± SEM are on the right. (c) n ≥ 4. (d) n = 6. (e) n ≥ 12. ns = not significant, ***p < 0.001.

Figure 8: *S*-acylation of EGFP-SNAP25B by zDHHC3 TMD3 mutants.
HEK293T cells were transfected with EGFP-SNAP25B and pEF-BOS-HA (*vector*) or the indicated wild-type or mutant zDHHC constructs. Cells were then incubated with C14:0, C16:0 or C18:0 fatty acid azides for 4h at 37 ºC. Fatty acid azides were labelled by click chemistry using an alkyne-800 infrared dye. Isolated proteins were resolved by SDS-PAGE and transferred to nitrocellulose membranes. (a) Sequence alignment of amino acids in the third transmembrane domain of zDHHC3 and zDHHC7; the blue boxes highlight Isoleucine-182 in zDHHC3 and Serine-185 in zDHHC7. (b) and (c) Analysis of EGFP-SNAP25B *S*-acylation by zDHHC3 TMD3 mutants with fatty acid-azides. Representative images are shown on the left, graphs showing mean ± SEM are on the right. (b) n ≥ 6. (c) n ≥ 8. ns = not significant, ***p < 0.001.

Figure 9: Incorporation of [^{3}H]palmitic and [^{3}H]stearic acid into EGFP-SNAP25B by zDHHC3 and zDHHC7.
HEK293T cells were transfected with pEGFPC2 or EGFP-SNAP25B together with pEF-BOS-HA (*vector*), HA-zDHHC3, HA-zDHHC7, or HA-zDHHC3(I182S). Cells were labelled with either [^{3}H]palmitic acid (Left panel) or [^{3}H]stearic acid (Right panel), lysed, and resolved by SDS-PAGE. Top panel: [^{3}H] fatty acid incorporation. Upper middle panel: expression levels of EGFP-SNAP25B. Lower middle panel: zDHHC protein expression. Molecular weight markers are shown on the left. Lower panel: Quantification of [^{3}H]fatty acid incorporation normalised to EGFP-SNAP25B protein levels expressed as mean ± SEM. n = 3, ns = not significant. **p < 0.01; ***p < 0.001.

FIGURE 1

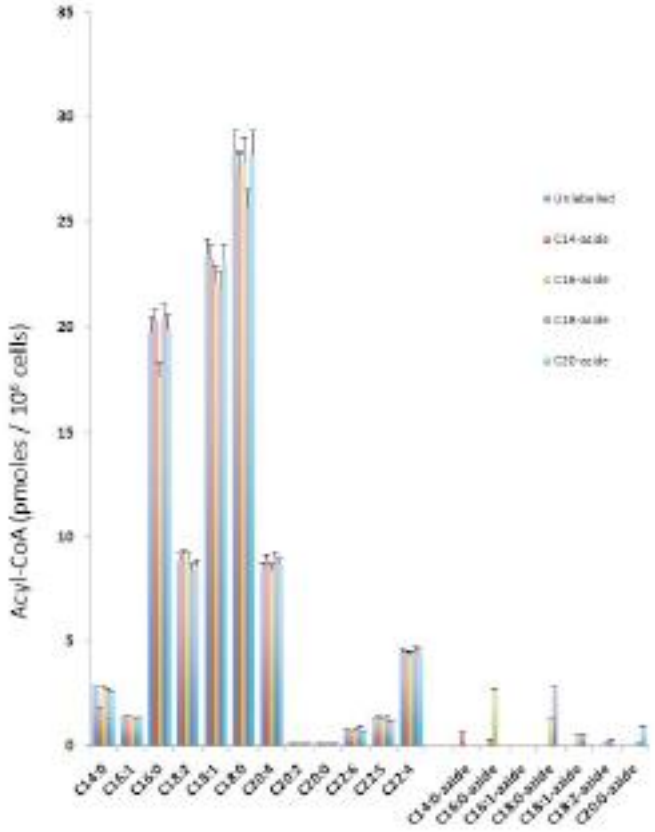
Acyl-CoA (pmoles / 10⁶ cells)
35
30
25
20
15
10
5
0
C14:0
C16:1
C16:0
C18:2
C18:1
C18:0
C20:4
C20:3
C20:0
C22:6
C22:5
C22:4
C14:0-aldehyde
C16:0-aldehyde
C18:1-aldehyde
C18:0-aldehyde
C18:1-aldehyde
C18:2-aldehyde
C20:0-aldehyde

FIGURE 2

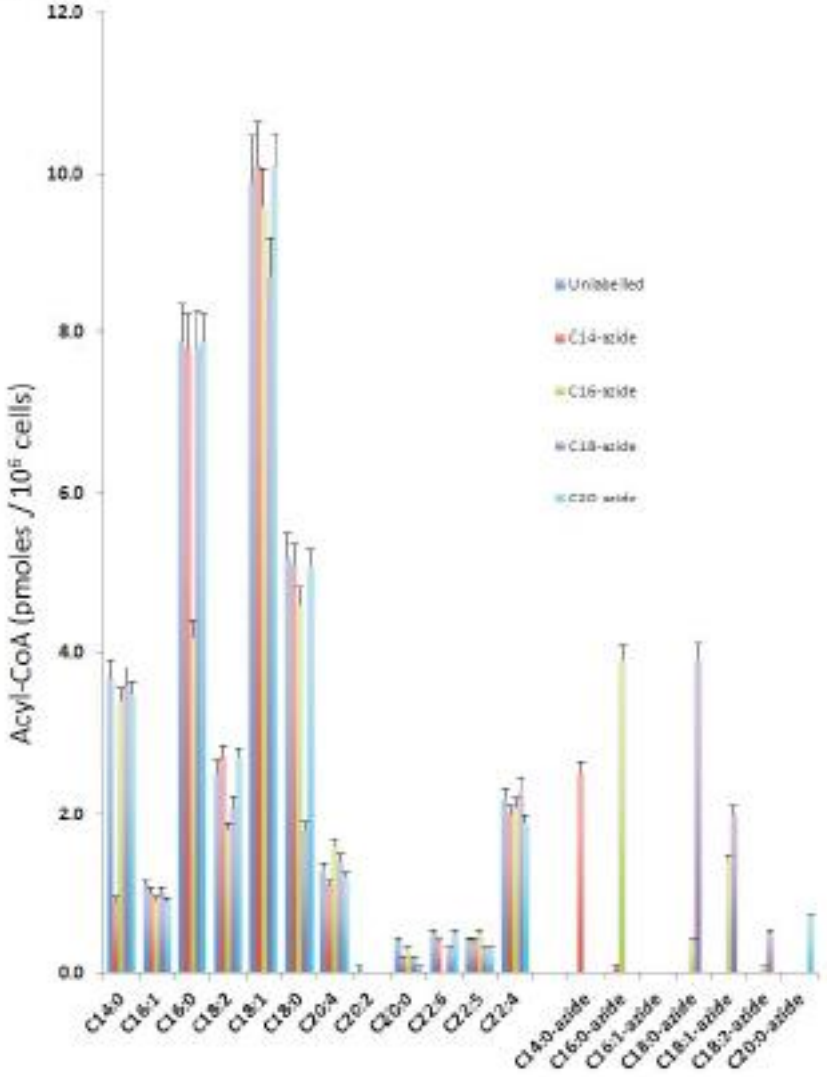
12.0
10.0
8.0
6.0
4.0
2.0
0.0
Acyl-CoA (pmoles / 10^6 cells)
Unlabelled
C14-azide
C16-azide
C18-azide
C20-azide
C14:0
C18:1
C16:0
C18:2
C18:3
C18:0
C20:4
C20:2
C20:0
C22:6
C22:5
C22:4
C14:0-azide
C16:0-azide
C16:1-azide
C18:0-azide
C18:1-azide
C18:2-azide
C20:0-azide

FIGURE 3

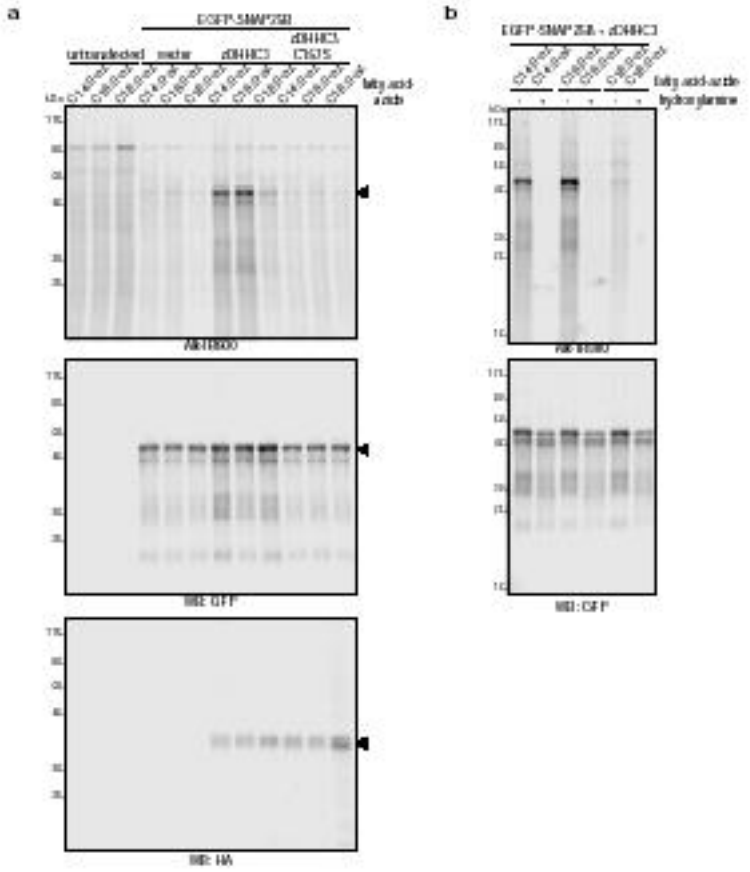

FIGURE 4

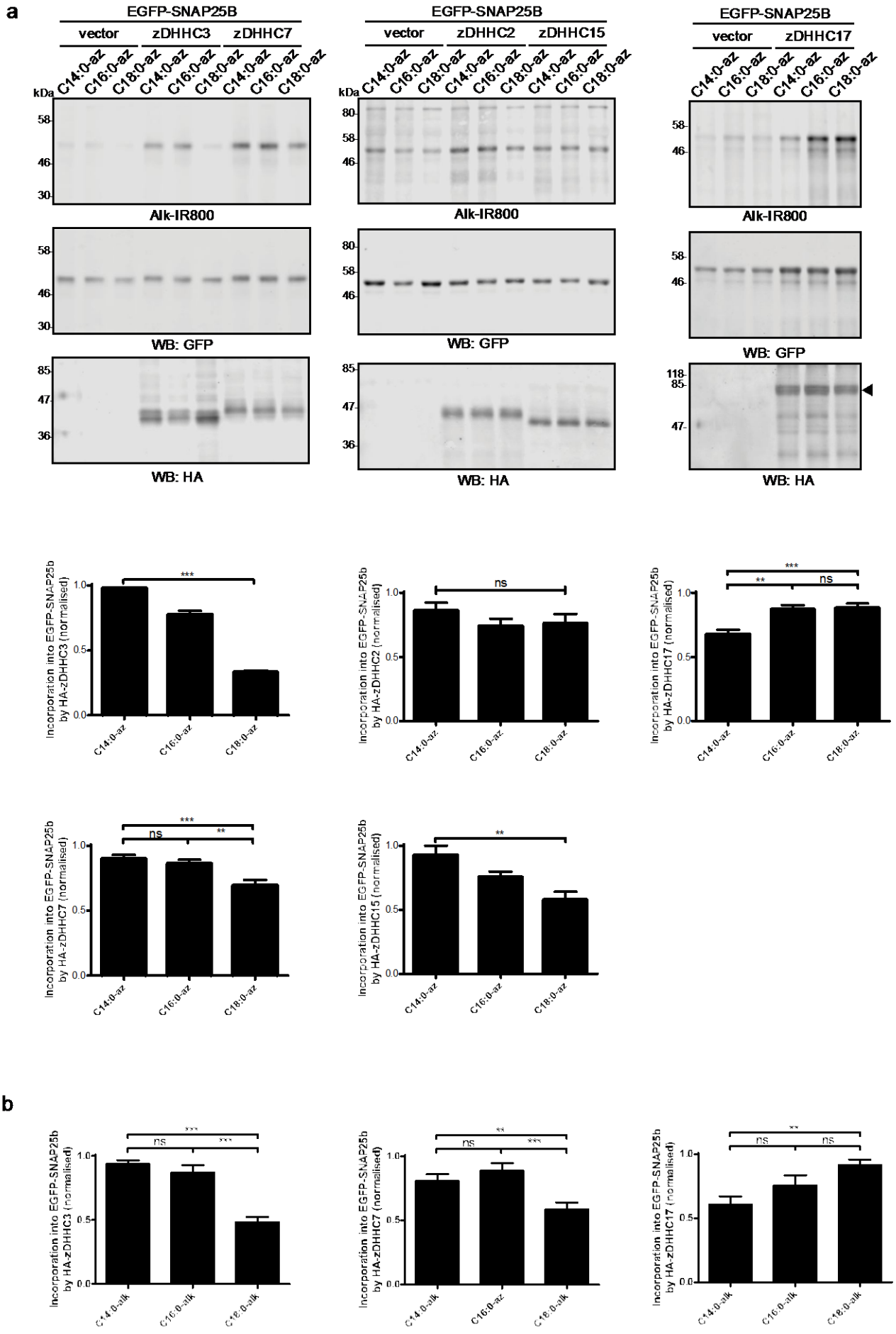
a
EGFP-SNAP25B
vector
zDHHC3
zDHHC7
zDHHC2
zDHHC15
zDHHC17
C14:0-az
C16:0-az
C18:0-az
kDa
Alk-IR800
WB: GFP
WB: HA
Incorporation into EGFP-SNAP25b by HA-zDHHC3 (normalised)
Incorporation into EGFP-SNAP25b by HA-zDHHC2 (normalised)
Incorporation into EGFP-SNAP25b by HA-zDHHC17 (normalised)
Incorporation into EGFP-SNAP25b by HA-zDHHC7 (normalised)
Incorporation into EGFP-SNAP25b by HA-zDHHC15 (normalised)
b
C14:0-alk
C16:0-alk
C18:0-alk

FIGURE 5

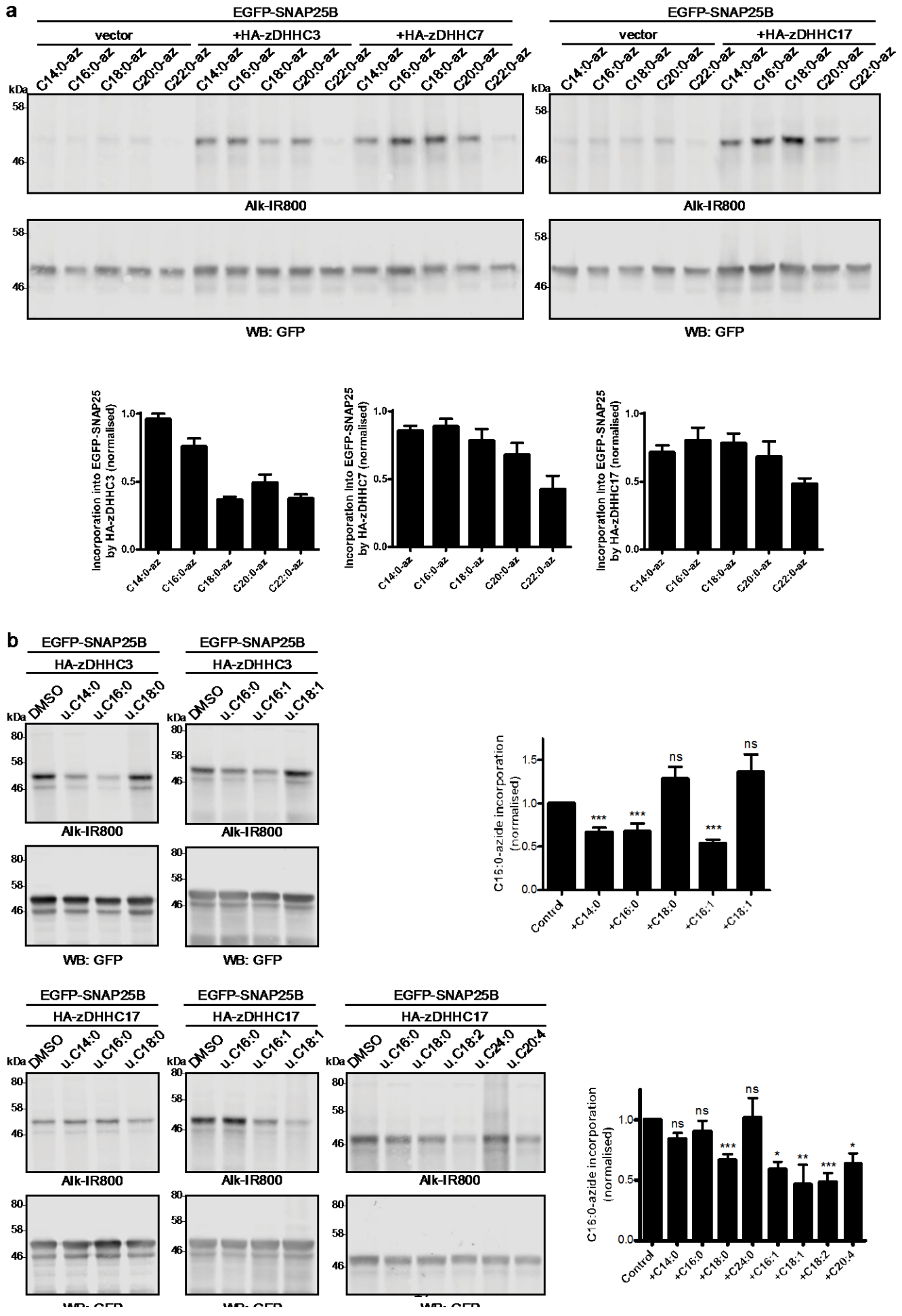
a
EGFP-SNAP25B
vector
+HA-zDHHC3
+HA-zDHHC7
+HA-zDHHC17
C14:0-az
C16:0-az
C18:0-az
C20:0-az
C22:0-az
kDa
58
46
Alk-IR800
WB: GFP
Incorporation into EGFP-SNAP25 by HA-zDHHC3 (normalised)
Incorporation into EGFP-SNAP25 by HA-zDHHC7 (normalised)
Incorporation into EGFP-SNAP25 by HA-zDHHC17 (normalised)
1.0
0.5
0.0
b
HA-zDHHC3
DMSO
u.C14:0
u.C16:0
u.C18:0
u.C16:1
u.C18:1
HA-zDHHC17
u.C18:2
u.C24:0
u.C20:4
C16:0-azide incorporation (normalised)
1.5
ns
***
Control
+C14:0
+C16:0
+C18:0
+C16:1
+C18:1
+C18:2
+C20:4
+C24:0
*
**

FIGURE 6

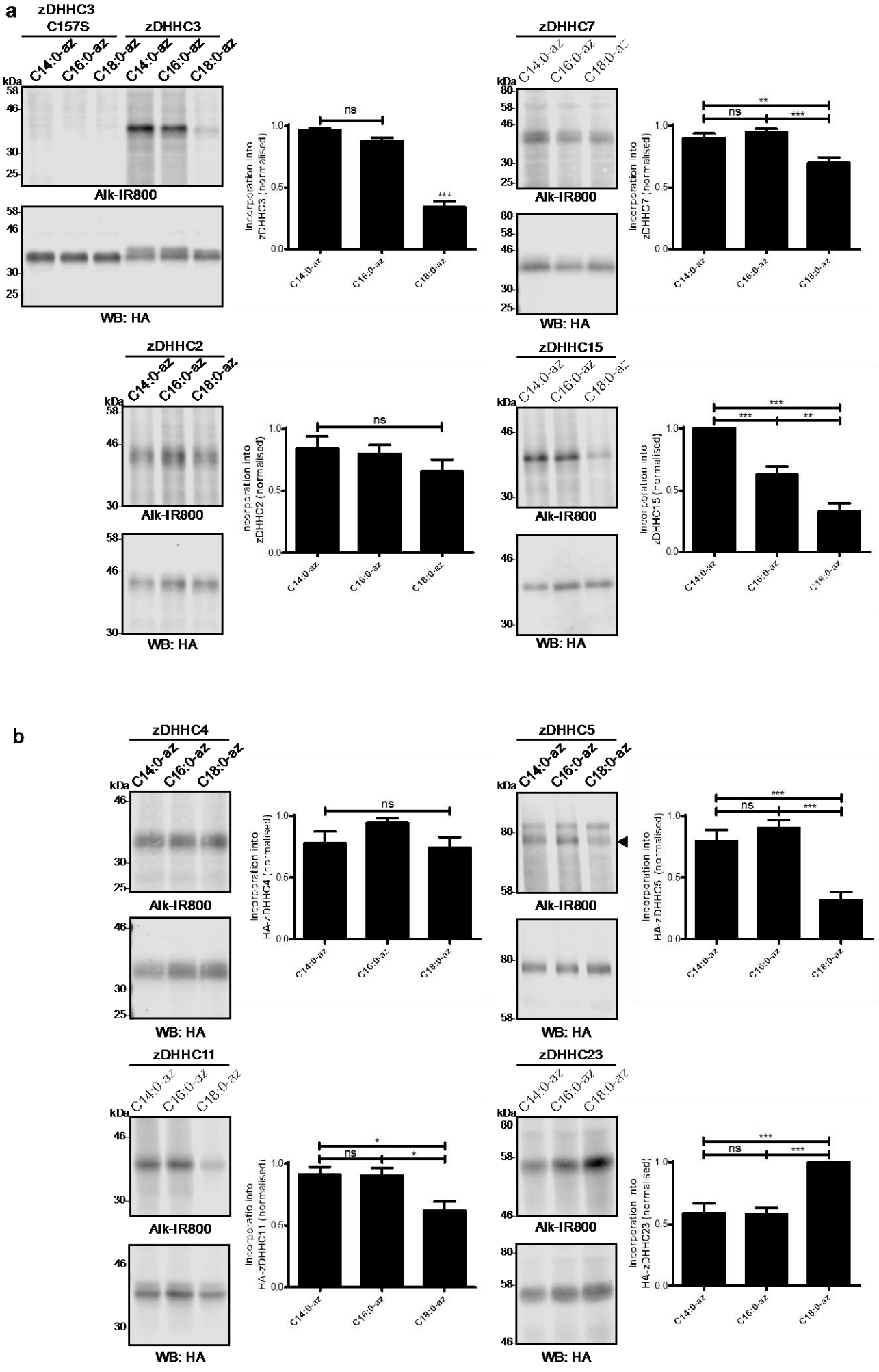
a
zDHHC3 C157S
zDHHC3
C14:0-az
C16:0-az
C18:0-az
kDa
Alk-IR800
WB: HA
Incorporation into zDHHC3 (normalised)
zDHHC7
Incorporation into zDHHC7 (normalised)
zDHHC2
Incorporation into zDHHC2 (normalised)
zDHHC15
Incorporation into zDHHC15 (normalised)
ns
b
zDHHC4
Incorporation into HA-zDHHC4 (normalised)
zDHHC5
Incorporation into HA-zDHHC5 (normalised)
zDHHC11
Incorporation into HA-zDHHC11 (normalised)
zDHHC23
Incorporation into HA-zDHHC23 (normalised)

FIGURE 7

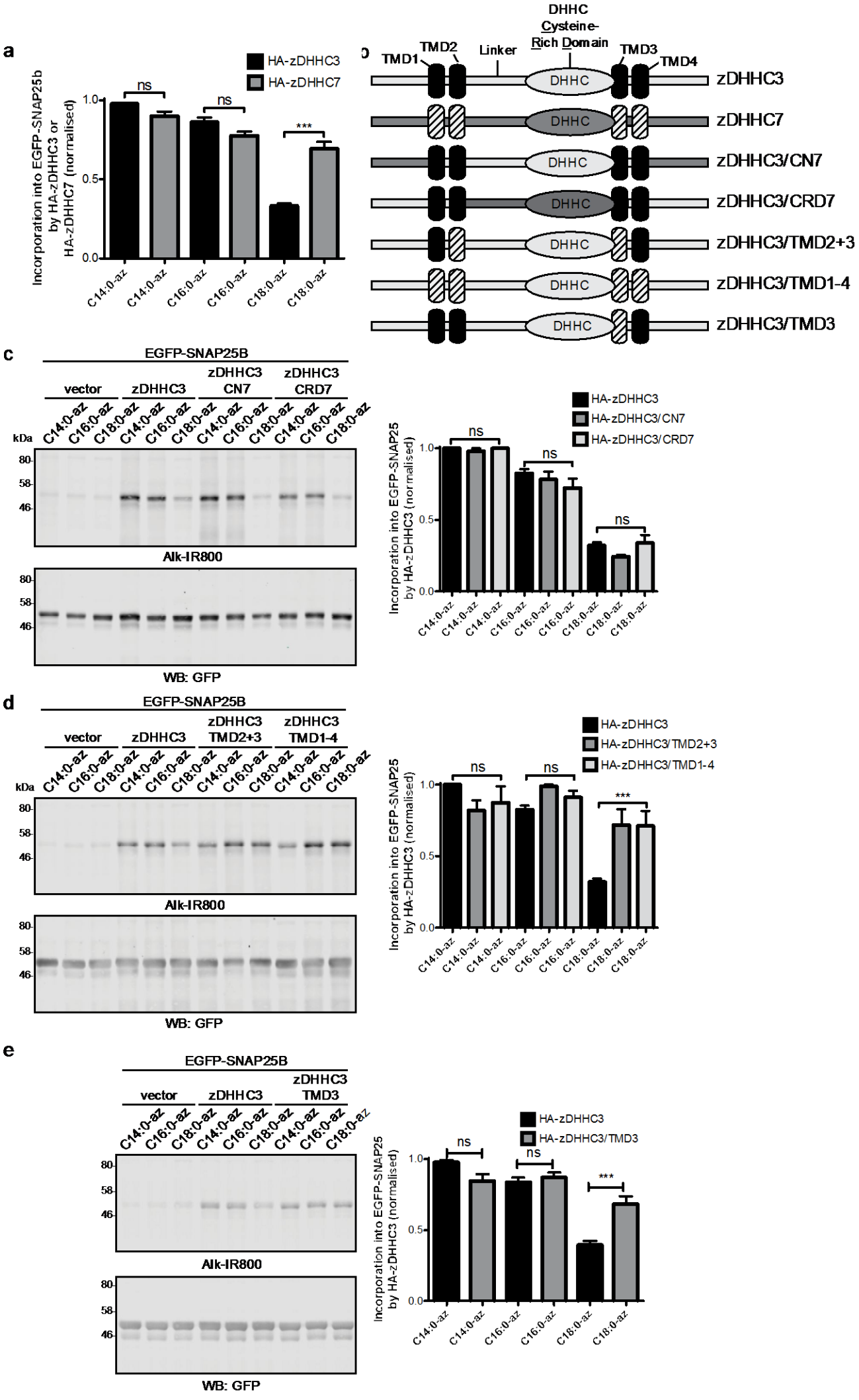
a
HA-zDHHC3
HA-zDHHC7
Incorporation into EGFP-SNAP25b by HA-zDHHC3 or HA-zDHHC7 (normalised)
ns
ns
***
C14:0-az
C14:0-az
C16:0-az
C16:0-az
C18:0-az
C18:0-az
b
DHHC Cysteine-Rich Domain
TMD1
TMD2
Linker
TMD3
TMD4
DHHC
zDHHC3
zDHHC7
zDHHC3/CN7
zDHHC3/CRD7
zDHHC3/TMD2+3
zDHHC3/TMD1-4
zDHHC3/TMD3
c
EGFP-SNAP25B
vector
zDHHC3
zDHHC3 CN7
zDHHC3 CRD7
kDa
Alk-IR800
WB: GFP
HA-zDHHC3
HA-zDHHC3/CN7
HA-zDHHC3/CRD7
Incorporation into EGFP-SNAP25 by HA-zDHHC3 (normalised)
d
EGFP-SNAP25B
vector
zDHHC3
zDHHC3 TMD2+3
zDHHC3 TMD1-4
Alk-IR800
WB: GFP
HA-zDHHC3
HA-zDHHC3/TMD2+3
HA-zDHHC3/TMD1-4
Incorporation into EGFP-SNAP25 by HA-zDHHC3 (normalised)
e
EGFP-SNAP25B
vector
zDHHC3
zDHHC3 TMD3
Alk-IR800
WB: GFP
HA-zDHHC3
HA-zDHHC3/TMD3
Incorporation into EGFP-SNAP25 by HA-zDHHC3 (normalised)

FIGURE 8

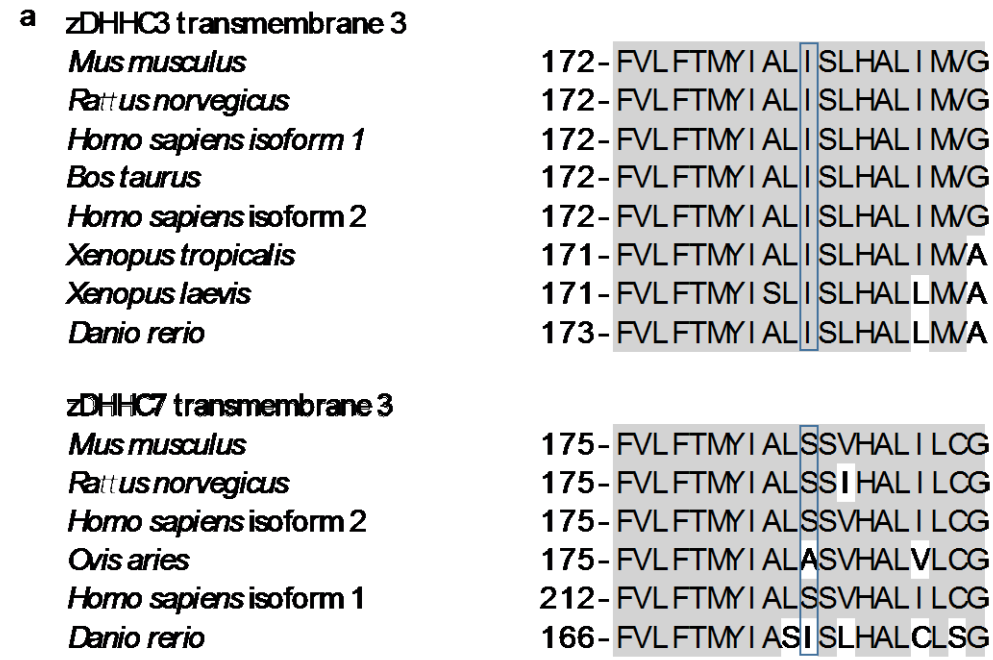
a
zDHHC3 transmembrane 3
Mus musculus 172-FVLFTMYIALISLHALIM/G
Rattus norvegicus 172-FVLFTMYIALISLHALIM/G
Homo sapiens isoform 1 172-FVLFTMYIALISLHALIM/G
Bos taurus 172-FVLFTMYIALISLHALIM/G
Homo sapiens isoform 2 172-FVLFTMYIALISLHALIM/G
Xenopus tropicalis 171-FVLFTMYIALISLHALIM/A
Xenopus laevis 171-FVLFTMYISLISLHALLM/A
Danio rerio 173-FVLFTMYIALISLHALLM/A
zDHHC7 transmembrane 3
Mus musculus 175-FVLFTMYIALSSVHALILCG
Rattus norvegicus 175-FVLFTMYIALSSIHALILCG
Homo sapiens isoform 2 175-FVLFTMYIALSSVHALILCG
Ovis aries 175-FVLFTMYIALASVHALVLCG
Homo sapiens isoform 1 212-FVLFTMYIALSSVHALILCG
Danio rerio 166-FVLFTMYIASISLHALCLSG

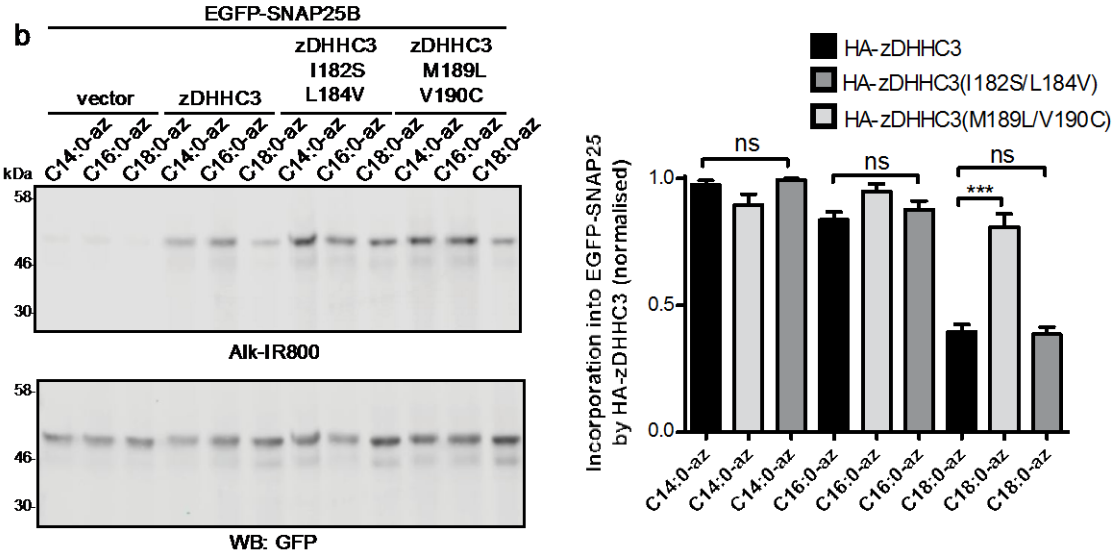
b
EGFP-SNAP25B
vector
zDHHC3
zDHHC3 I182S L184V
zDHHC3 M189L V190C
C14:0-az
C16:0-az
C18:0-az
kDa
58
46
30
Alk-IR800
WB: GFP
HA-zDHHC3
HA-zDHHC3(I182S/L184V)
HA-zDHHC3(M189L/V190C)
Incorporation into EGFP-SNAP25 by HA-zDHHC3 (normalised)
ns
***
1.0
0.5
0.0

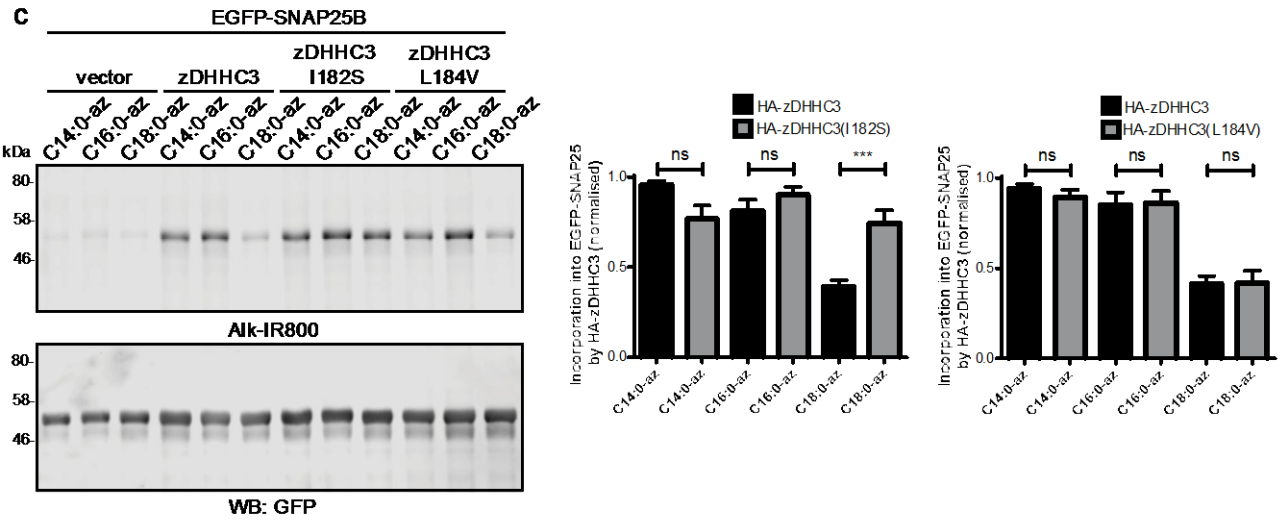
c
EGFP-SNAP25B
vector
zDHHC3
zDHHC3 I182S
zDHHC3 L184V
C14:0-az
C16:0-az
C18:0-az
kDa
80
58
46
Alk-IR800
WB: GFP
HA-zDHHC3
HA-zDHHC3(I182S)
HA-zDHHC3(L184V)
Incorporation into EGFP-SNAP25 by HA-zDHHC3 (normalised)
ns
***
1.0
0.5
0.0

FIGURE 9

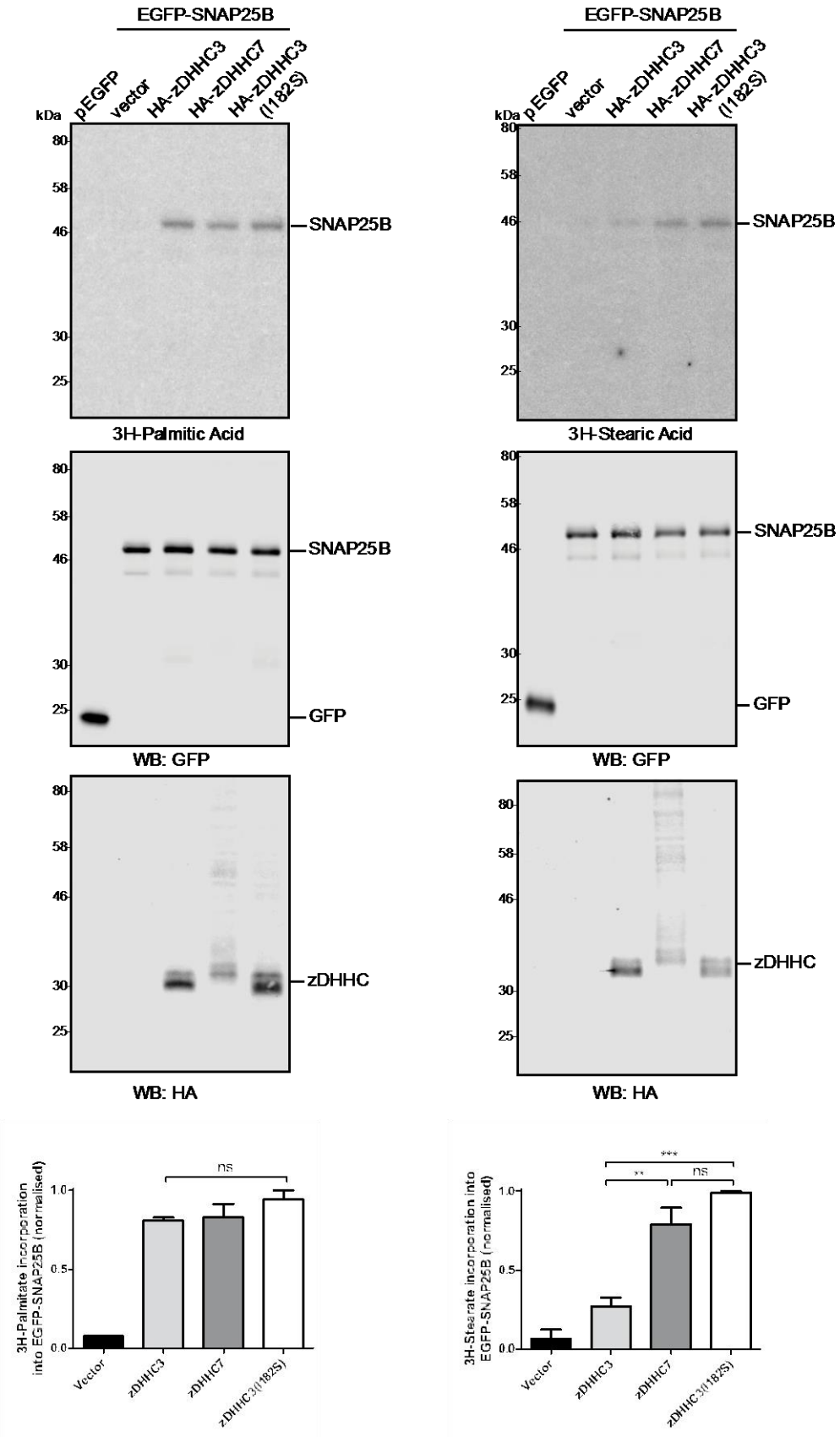
EGFP-SNAP25B
pEGFP
vector
HA-zDHHC3
HA-zDHHC7
HA-zDHHC3 (I182S)
kDa
80
58
46
30
25
SNAP25B
3H-Palmitic Acid
3H-Stearic Acid
GFP
WB: GFP
zDHHC
WB: HA
3H-Palmitate incorporation into EGFP-SNAP25B (normalised)
3H-Stearate incorporation into EGFP-SNAP25B (normalised)
ns
**
***
1.0
0.5
0.0
Vector
zDHHC3
zDHHC7
zDHHC3(I182S)

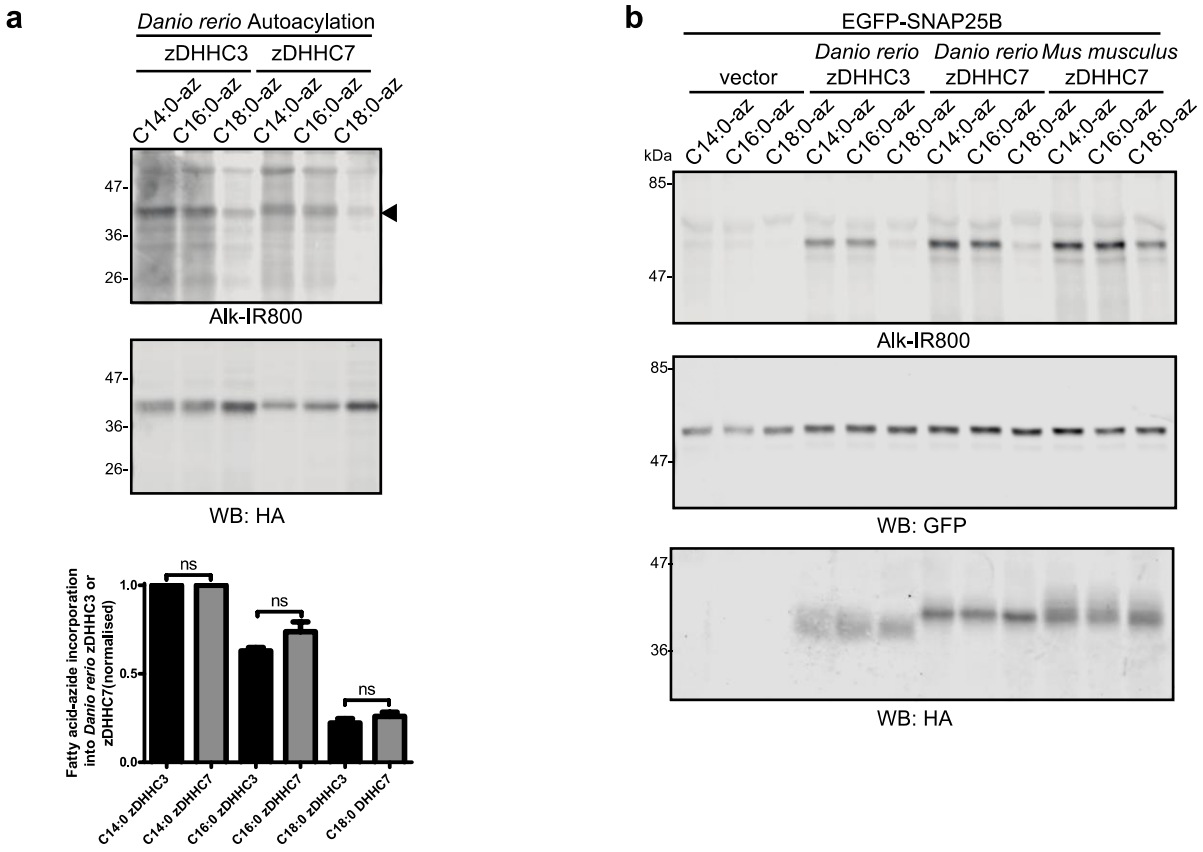

Supplementary Figure 3: S-acylation profiles of *Danio rerio* zDHHC3 and zDHHC7 by fatty-acid azides.
(A) HEK293T cells transfected with HA-tagged zDHHC3 or zDHHC7 from *Danio rerio* were incubated with C14:0, C16:0 or C18:0 fatty acid azides for 4 h at 37 ºC. Fatty acid azides were then labelled by click chemistry using an alkyne-800 infrared dye. Isolated proteins were resolved by SDS-PAGE and transferred to nitrocellulose membranes. Representative click signals and western blots and quantified data (mean ± SEM) are shown. n = 5; ns = not significant. (B) HEK293T cells were transfected with EGFP-SNAP25B together with either pEF-BOS-HA (vector control), zDHHC3 or zDHHC7 from *Danio rerio*, or mouse zDHHC7. Cells were then incubated with C14:0, C16:0 or C18:0 fatty acid azides for 4 h at 37 ºC, and fatty acid azides were then labelled by click chemistry using an alkyne-800 infrared dye. Isolated proteins were resolved by SDS-PAGE and transferred to nitrocellulose membranes. Representative click signals and western blots are shown.